CHAPTER 4

RING-OPENING POLYMERISATIONS : KINETIC STUDIES

In this part of the work, the actual kinetics of the type of ring-opening polymerisation reactions described in the previous chapter were studied in more detail. However, this was not intended to be a comprehensive study of all the cyclic esters, merely a comparative study of just 2 of them. The monomers and reaction conditions that were chosen for this study were:

MONOMERS : δ-valerolactone and ε-caprolactone
INITIATOR : stannous octoate (0.1 mole %)
TEMPERATURES : 80°C and 90°C (isothermal)
TECHNIQUES : dilatometry, gravimetry, viscometry

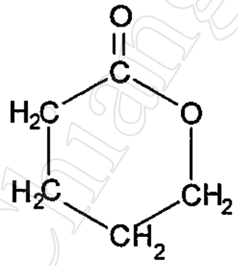

δ-valerolactone

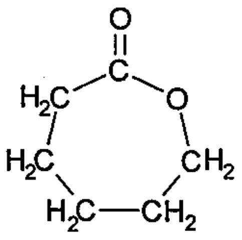

ε-caprolactone

δ-Valerolactone and ε-caprolactone were chosen because of their easy polymerisability and the fact that not only they but also their polymers are liquids at the temperatures used. This avoided the problem of solidification occurring during the course of the experiments. The experiments were conducted isothermally in a thermostatically controlled, circular, glass water bath with a temperature variation of less than ±0.1°C.

4.1 Dilatometry

4.1.1 Dilatometer Design and Calibration

For following the volume change during polymerisation, the reaction was carried out in a dilatometer, as shown in Fig. 4.1. The design and construction of these small glass instruments depend on a number of considerations, such as the expected volume change and the accuracy with which it must be measured, the rate of polymerisation, the corresponding rate of heat evolution and its effect on temperature uniformity, the viscosity of the polymerising mixture, and the need for stirring. If, as is usual, a capillary is used to display the volume change, good temperature control throughout is essential, if possible to within ±0.01°C, since the dilatometer is effectively also a very sensitive thermometer.

Before use, it was first necessary to calibrate the dilatometer with respect to its volumetric dimensions. This was done by weighing the dilatometer empty and then filled with a known weight of monomer such that the meniscus level came within the capillary range at the temperature of the experiment. The density of the monomer at this temperature had already been determined in a density bottle equipped with a thermometer, while the capillary diameter was measured microscopically from a thinly-cut cross-section.

Fig. 4.1 : Dilatometer used in kinetic studies.

4.1.2 Experimental Procedure and Results

An appropriate amount of distilled, degassed monomer together with 0.1 mole % of stannous octoate were accurately weighed into a 10 ml 'Quickfit' conical flask. A small magnetic bar was added and the capillary inserted into the neck of the flask so that the monomer meniscus level rose to a suitable height in the capillary. The complete dilatometer assembly was then clamped accurately vertical in the water bath at the polymerisation temperature (zero time, t = 0), a stop-watch started, and a cathetometer focussed on the monomer meniscus level. Thereafter, the meniscus level was read at regular intervals, short at the beginning and then lengthening as the time progressed.

From the cathetometer scale readings of meniscus height (h) obtained as a function of time (t), the % conversion and rate of polymerisation (r_p) were calculated from the equations:

$$\% \text{ conversion} = \frac{100\Delta V}{V_o - V_\infty} = \frac{100\Delta h(t)}{\Delta h(t=\infty)}$$

$$r_p = \frac{\Delta h(t)}{\Delta h(t=\infty)} \frac{[M]_o}{t}$$

At the end of the polymerisation, when the meniscus height had become constant, the contents of the dilatometer were dissolved in chloroform and the polymer precipitated in absolute ethanol for gravimetric determination. The gravimetric final % conversion (at t = ∞) thus obtained provided some indication as to the validity of the assumption used in the dilatometric rate analysis that $\Delta h(t = \infty)$ corresponded to 100% conversion.

4.1.2.1 δ-Valerolactone

The experimental results for the δ-valerolactone polymerisations at 80°C and 90°C are given in Tables 4.1 and 4.2 respectively. From these results, the corresponding graphs of meniscus height, h, % conversion and rate of polymerisation, r_p, are plotted against time, as shown in Figs. 4.2-4.9. At the beginning of each polymerisation, there was a short thermal equilibration period (≈ 3 mins) during which the meniscus level rose in the capillary due to thermal expansion. Consequently, the hypothetical meniscus height at zero time, h_0, at the actual polymerisation temperature, as required in the above % conversion and rate calculations, could only be estimated by extrapolation back to time $t = 0$ of the raw data plot between h and t.

Table 4.1 : Dilatometric data from δ-valerolactone polymerisation at 80°C.

weight of δ-valerolactone = 14.7369 g
weight of stannous octoate = 0.0608 g
capillary diameter = 0.180 cm
h_0 (from extrapolation in Fig. 4.3) = 27.320 cm

Time (mins)	h (cm)	Conversion (%)	r_p (mol/l·min)
1	26.240	thermal equilibration	
2	27.240		
3	27.290		
4	27.295	0.12	0.00317
5	27.274	0.22	0.00467
8	27.265	0.27	0.00349
12	27.245	0.36	0.00317
18	27.225	0.46	0.00268
26	27.175	0.70	0.00283
40	27.100	1.06	0.00279
51	27.030	1.40	0.00289
60	26.960	1.74	0.00305
80	26.820	2.41	0.00317
100	26.665	3.16	0.00333
120	26.500	3.96	0.00347
140	26.315	4.85	0.00365
160	26.115	5.81	0.00382
180	25.932	6.70	0.00392
200	25.700	7.82	0.00411
220	25.510	8.73	0.00418
240	25.290	9.80	0.00429
260	25.078	10.82	0.00438
280	24.850	11.92	0.00448
300	24.605	13.10	0.00460
315	24.300	14.57	0.00487
340	24.155	15.27	0.00473
360	23.900	16.50	0.00482
380	23.675	17.59	0.00487
400	23.425	18.80	0.00494
420	23.245	19.66	0.00493
440	22.992	20.89	0.00499
460	22.617	22.69	0.00519
480	22.471	23.40	0.00513
500	22.240	24.51	0.00516
520	21.970	25.82	0.00522
540	21.700	27.12	0.00528
573	21.314	28.98	0.00532
626	20.645	32.21	0.00541
660	20.285	33.95	0.00541
690	19.900	35.81	0.00546
720	19.575	37.37	0.00546
750	19.230	39.04	0.00548
780	18.885	40.70	0.00549
796	18.665	41.77	0.00552
842	18.220	43.91	0.00549
900	17.615	46.83	0.00548
1020	16.360	52.89	0.00546
1140	15.750	55.83	0.00515

Table 4.1 : continued

Time (mins)	h (cm)	Conversion (%)	r_p (mol/l·min)
1200	14.705	60.87	0.00534
1260	14.220	63.21	0.00528
1320	13.765	65.41	0.00521
1380	13.345	67.44	0.00514
1440	12.920	69.49	0.00508
1498	12.580	71.13	0.00500
1560	12.175	73.08	0.00493
1680	11.515	76.27	0.00478
1805	10.990	78.80	0.00459
1920	10.530	81.02	0.00444
1980	10.300	82.13	0.00436
2100	9.985	83.65	0.00419
2280	9.460	86.18	0.00398
2640	8.705	89.83	0.00358
2865	8.335	91.61	0.00336
3180	7.925	93.59	0.00310
3580	7.575	95.28	0.00280
3640	7.524	95.53	0.00276
4177	7.230	96.95	0.00244
4361	7.150	97.33	0.00235
4502	7.100	97.57	0.00228
4658	7.050	97.81	0.00221
4897	7.000	98.06	0.00211
5016	6.950	98.30	0.00206
5125	6.915	98.47	0.00202
5700	6.790	99.07	0.00183
5995	6.790	99.07	0.00174
6420	6.730	99.36	0.00163
7082	6.695	99.53	0.00148
7315	6.645	99.77	0.00144
7515	6.645	99.77	0.00140
7647	6.645	99.77	0.00137
7966	6.645	99.77	0.00132
8570	6.617	99.90	0.00123
8770	6.617	99.90	0.00120
8965	6.617	99.90	0.00117
9187	6.617	99.90	0.00114
9375	6.617	99.90	0.00112
10088	6.597	100.00	0.00104
10308	6.597	100.00	0.00102
10508	6.597	100.00	0.00100
10830	6.597	100.00	0.00097
11490	6.597	100.00	0.00092
11520	6.597	100.00	0.00091

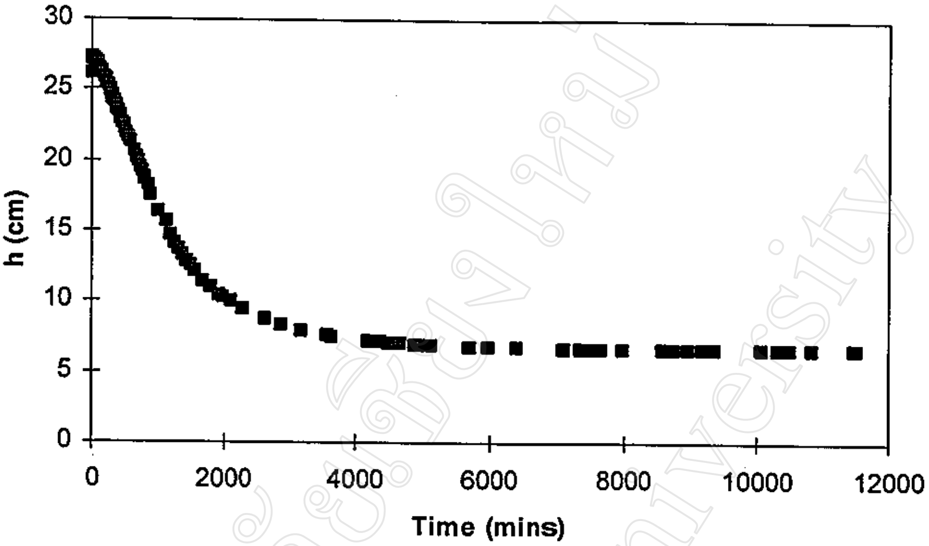

Fig. 4.2 : Graph of meniscus height, h, against time for δ-valerolactone polymerisation at 80°C.

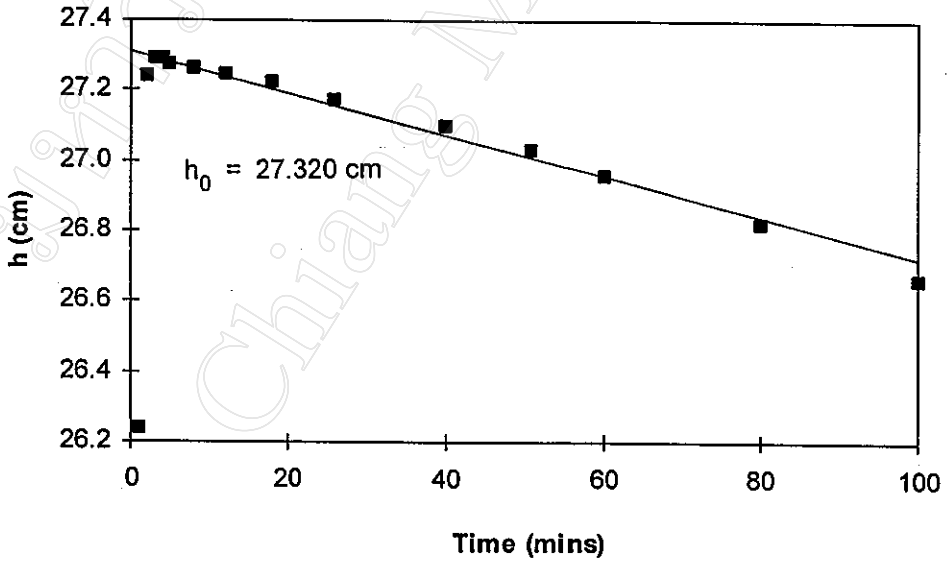

Fig. 4.3 : Extrapolation of h to zero time (h_0 at t = 0) for δ-valerolactone polymerisation at 80°C.

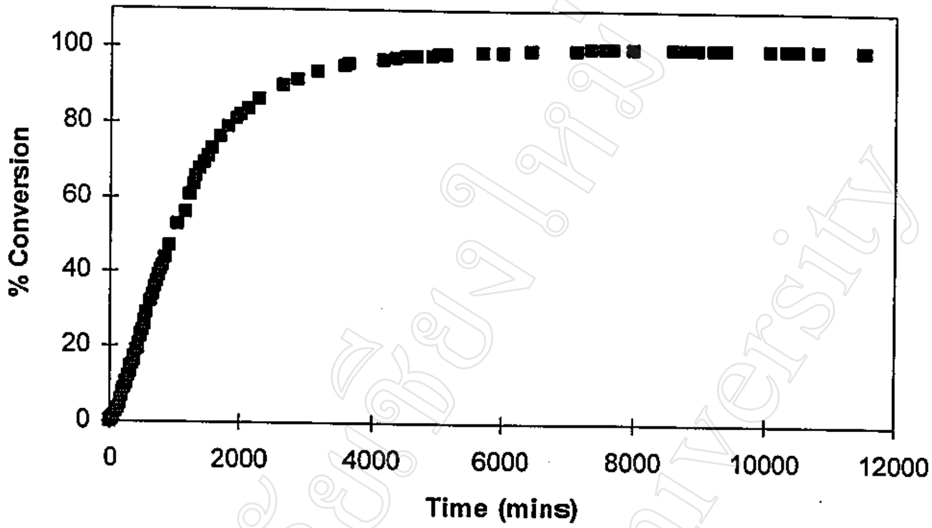

Fig. 4.4 : Kinetic profile from dilatometry of % conversion against time for δ-valerolactone polymerisation at 80°C.

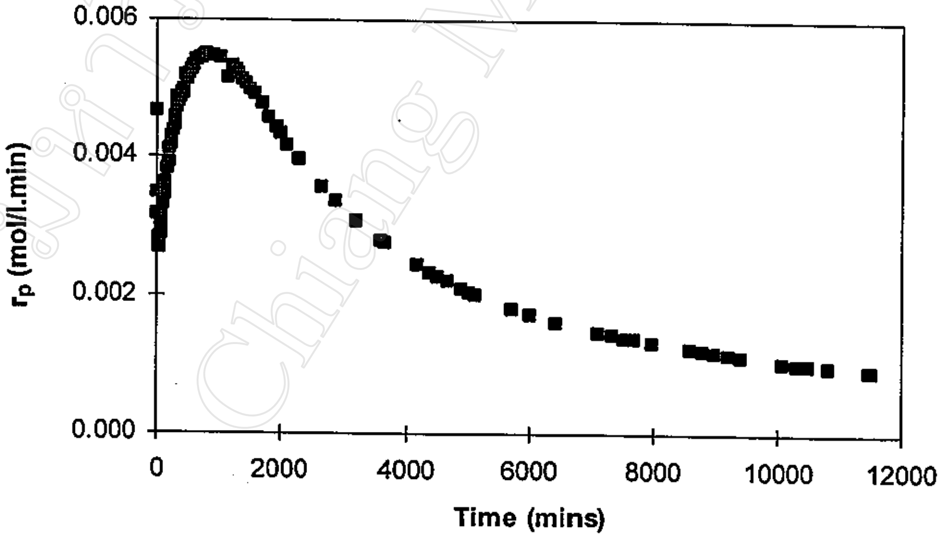

Fig. 4.5 : Kinetic profile from dilatometry of the rate of polymerisation, r_p , against time for δ-valerolactone polymerisation at 80°C.

Table 4.2 : Dilatometric data from δ-valerolactone polymerisation at 90°C.

weight of δ-valerolactone = 14.6280 g
weight of stannous octoate = 0.0593 g
capillary diameter = 0.180 cm
h_0 (from extrapolation in Fig. 4.7) = 28.820 cm

Time (mins)	h (cm)	Conversion (%)	r_p (mol/l·min)
3	28.785	0.16	0.00569
5	28.770	0.23	0.00488
8	28.720	0.47	0.00610
10	28.655	0.77	0.00805
15	28.605	1.01	0.00699
20	28.550	1.26	0.00658
30	28.425	1.85	0.00642
40	28.315	2.36	0.00616
50	28.205	2.88	0.00600
60	28.065	3.53	0.00614
72	27.920	4.21	0.00610
82	27.760	4.96	0.00631
91	27.630	5.56	0.00638
100	27.490	6.22	0.00649
110	27.340	6.92	0.00656
120	27.150	7.81	0.00679
140	26.830	9.30	0.00693
160	26.445	11.10	0.00724
180	26.120	12.62	0.00732
200	25.735	14.42	0.00752
220	25.380	16.08	0.00763
240	24.965	18.02	0.00783
260	24.575	19.85	0.00796
280	24.120	21.97	0.00819

Time (mins)	h (cm)	Conversion (%)	r_p (mol/l·min)
300	23.730	23.80	0.00828
320	23.340	25.62	0.00835
340	22.915	27.61	0.00847
360	22.515	29.48	0.00854
382	22.090	31.47	0.00859
400	21.700	33.29	0.00868
420	21.350	34.93	0.00868
440	20.980	36.66	0.00869
460	20.600	38.43	0.00872
480	20.215	40.23	0.00874
500	19.834	42.01	0.00877
520	19.635	42.94	0.00862
540	19.035	45.75	0.00884
560	18.645	47.57	0.00886
580	18.265	49.35	0.00888
600	17.895	51.08	0.00888
620	17.525	52.81	0.00889
640	17.150	54.56	0.00889
660	16.785	56.27	0.00889
683	16.410	58.02	0.00886
700	16.120	59.38	0.00885
720	15.790	60.92	0.00883
740	15.485	62.35	0.00879
760	15.165	63.84	0.00876

Table 4.2 : continued

Time (mins)	h (cm)	Conversion (%)	r_p (mol/l·min)
780	14.820	65.46	0.00875
810	14.465	67.12	0.00864
840	14.035	69.13	0.00859
870	13.690	70.74	0.00848
900	13.318	72.48	0.00840
930	12.990	74.01	0.00830
960	12.670	75.51	0.00821
990	12.395	76.80	0.00809
1020	12.100	78.17	0.00800
1080	11.615	80.44	0.00777
1140	11.175	82.50	0.00755
1200	10.840	84.07	0.00731
1260	10.450	85.89	0.00711
1320	10.170	87.20	0.00689
1380	9.920	88.37	0.00668
1440	9.695	89.42	0.00648
1500	9.450	90.56	0.00630
1560	9.290	91.31	0.00611
1577	9.225	91.62	0.00606
1680	8.955	92.88	0.00577
1800	8.740	93.88	0.00544
1920	8.500	95.01	0.00516
2030	8.330	95.80	0.00492
2157	8.190	96.46	0.00467
2334	8.035	97.18	0.00434
2695	7.777	98.39	0.00381
2795	7.735	98.58	0.00368
2927	7.698	98.76	0.00352
3195	7.584	99.29	0.00324
3346	7.510	99.64	0.00311
3480	7.485	99.75	0.00299
3731	7.485	99.75	0.00279
4250	7.432	100.00	0.00245
4330	7.432	100.00	0.00241
4618	7.432	100.00	0.00226
5075	7.432	100.00	0.00206
5673	7.432	100.00	0.00184
5760	7.432	100.00	0.00181

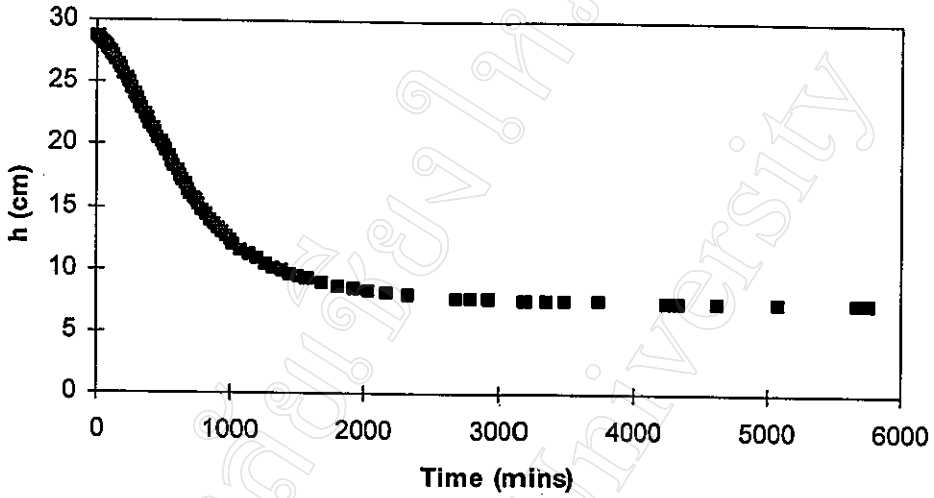

Fig. 4.6 : Graph of meniscus height, h, against time for δ-valerolactone polymerisation at 90°C.

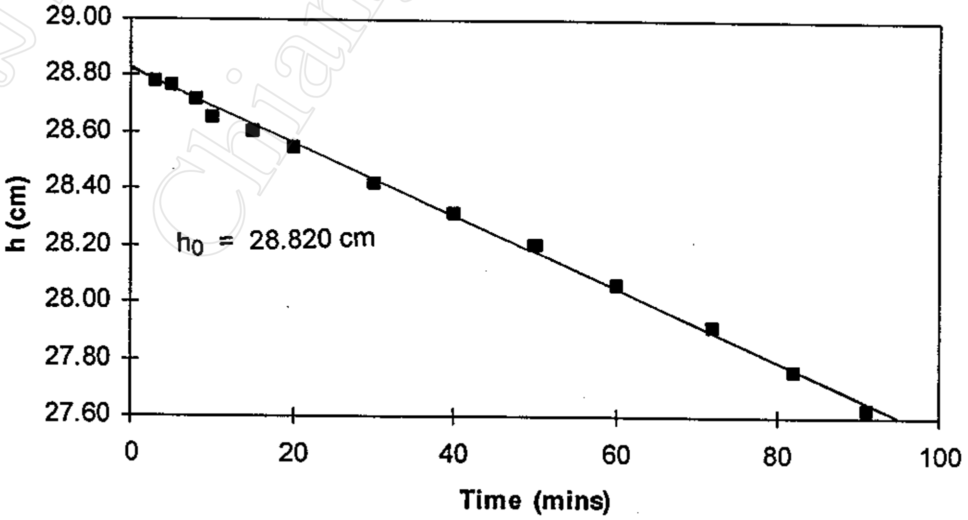

Fig. 4.7 : Extrapolation of h to zero time (h_0 at t = 0) for δ-valerolactone polymerisation at 90°C.

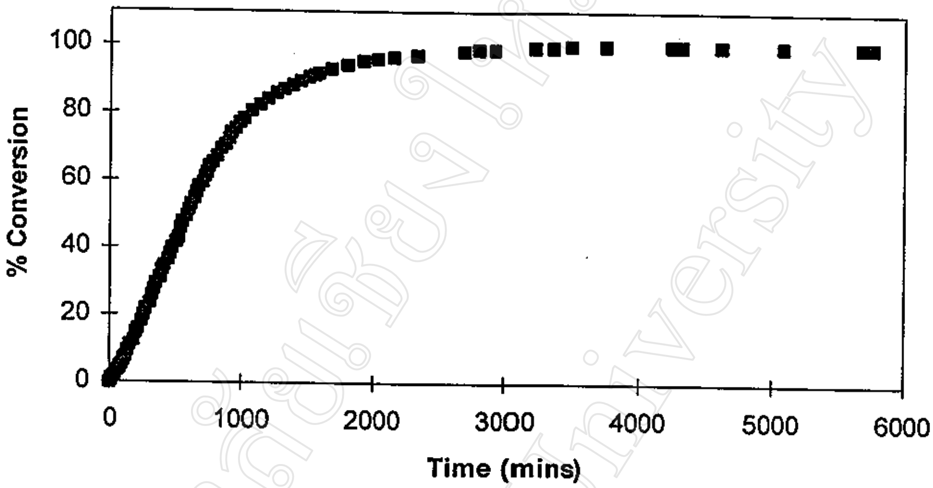

Fig. 4.8 : Kinetic profile from dilatometry of % conversion against time for δ-valerolactone polymerisation at 90°C.

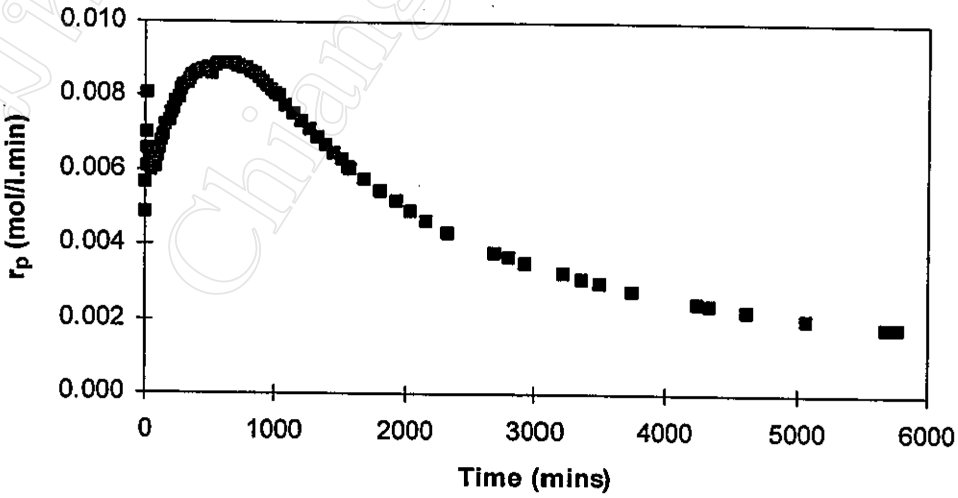

Fig. 4.9 : Kinetic profile from dilatometry of the rate of polymerisation, r_p , against time for δ-valerolactone polymerisation at 90°C.

4.1.2.2 ε-Caprolactone

Tables 4.3 and 4.4 show the dilatometric results for ε-caprolactone at 80°C and 90°C respectively. From these results, the corresponding graphs of meniscus height, h, % conversion and rate of polymerisation, r_p, are plotted against time, as shown in Figs. 4.10-4.17. At the beginning of each polymerisation, there was again a short thermal equilibration period (≈ 7 mins), slightly longer than for δ-valerolactone, during which the meniscus level initially increased in the capillary up to a maximum height before decreasing.

Table 4.3 : Dilatometric data from ε-caprolactone polymerisation at 80°C.

weight of ε-caprolactone = 14.4697 g
weight of stannous octoate = 0.0517 g
capillary diameter = 0.143 cm
h_0 (from extrapolation in Fig. 4.11) = 29.380 cm

Time (mins)	h (cm)	Conversion (%)	r_p (mol/l·min)
2	29.200	thermal equilibration	
3	29.330		
4	29.225		
5	29.336		
7	29.350	0.15	0.00192
10	29.345	0.17	0.00157
20	29.309	0.35	0.00159
30	29.214	0.83	0.00248
40	29.120	1.29	0.00291
50	29.090	1.44	0.00260
60	29.040	1.69	0.00254
80	29.000	1.89	0.00213
100	28.920	2.29	0.00206
120	28.905	2.37	0.00177
160	28.775	3.01	0.00169
180	28.700	3.39	0.00169
220	28.580	3.98	0.00163
240	28.465	4.56	0.00171
280	28.365	5.05	0.00162
300	28.275	5.50	0.00165
340	28.085	6.45	0.00170
365	27.990	6.92	0.00170
390	27.862	7.56	0.00174
425	27.675	8.49	0.00180
450	27.570	9.01	0.00180
480	27.410	9.81	0.00184

Table 4.3 : continued

Time (mins)	h (cm)	Conversion (%)	r_p (mol/l·min)
515	27.210	10.81	0.00189
540	27.240	10.66	0.00177
690	26.350	15.09	0.00197
720	26.105	16.31	0.00204
785	25.720	18.23	0.00209
900	24.900	22.31	0.00223
980	24.430	24.65	0.00226
1000	24.205	25.77	0.00232
1075	23.850	27.54	0.00230
1170	23.209	30.73	0.00236
1260	22.675	33.39	0.00238
1350	22.045	36.53	0.00243
1435	21.465	39.42	0.00247
1505	20.985	41.81	0.00250
1565	20.625	43.60	0.00250
1620	20.280	45.32	0.00251
1680	19.860	47.41	0.00254
1740	19.490	49.25	0.00254
1800	19.125	51.07	0.00255
1860	18.750	52.94	0.00256
1920	18.410	54.63	0.00256
1975	18.085	56.25	0.00256
2060	17.685	58.24	0.00254
2160	17.170	60.81	0.00253
2250	16.620	63.55	0.00254
2330	16.310	65.09	0.00251
2430	15.840	67.43	0.00249
2520	15.450	69.37	0.00247
2610	15.120	71.02	0.00245
2700	14.760	72.81	0.00242
2820	14.335	74.93	0.00239
2880	14.150	75.85	0.00237
3000	13.800	77.59	0.00232
3120	13.460	79.28	0.00228
3240	13.140	80.88	0.00224
3360	12.850	82.32	0.00220
3480	12.590	83.62	0.00216
3600	12.330	84.91	0.00212
3720	12.130	85.91	0.00208
3830	11.942	86.84	0.00204
3930	11.820	87.45	0.00200
4090	11.580	88.65	0.00195
4140	11.510	88.99	0.00193
4320	11.319	89.95	0.00187
4500	11.120	90.94	0.00182
4680	10.825	92.41	0.00177
4800	10.825	92.41	0.00173
4980	10.700	93.03	0.00168
5170	10.650	93.28	0.00162
5550	10.350	94.77	0.00153
5790	10.285	95.09	0.00148
6080	10.125	95.89	0.00142
6270	10.088	96.08	0.00138
6405	10.010	96.46	0.00135

Table 4.3 : continued

Time (mins)	h (cm)	Conversion (%)	r_p (mol/l·min)
6595	9.985	96.59	0.00132
6990	9.890	97.06	0.00125
7230	9.839	97.32	0.00121
7955	9.725	97.88	0.00111
8575	9.625	98.38	0.00103
8950	9.615	98.43	0.00099
9100	9.598	98.52	0.00097
10020	9.500	99.00	0.00089
10240	9.500	99.00	0.00087
10795	9.500	99.00	0.00082
11450	9.435	99.33	0.00078
12160	9.435	99.33	0.00073

Time (mins)	h (cm)	Conversion (%)	r_p (mol/l·min)
12915	9.385	99.58	0.00069
13505	9.375	99.63	0.00066
14315	9.340	99.80	0.00063
15155	9.330	99.85	0.00059
15745	9.330	99.85	0.00057
15960	9.300	100.00	0.00056
17195	9.300	100.00	0.00052
17410	9.300	100.00	0.00052
17545	9.300	100.00	0.00051
18060	9.300	100.00	0.00050
18720	9.300	100.00	0.00048

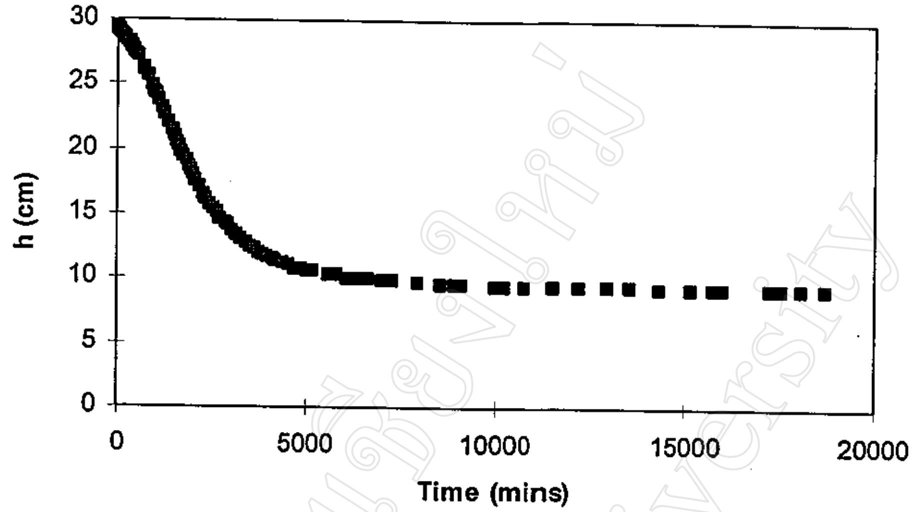

Fig. 4.10 : Graph of meniscus height, h, against time for ε-caprolactone polymerisation at 80°C.

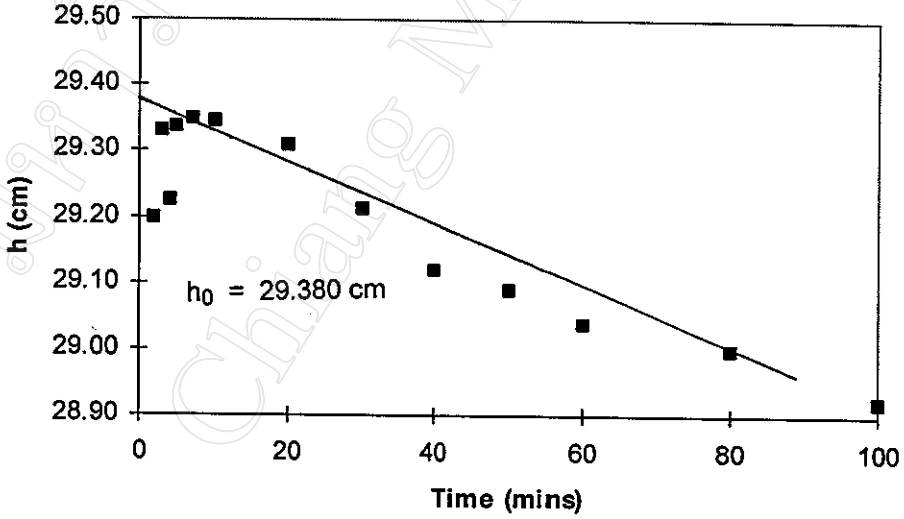

Fig. 4.11 : Extrapolation of h to zero time (h_0 at t = 0) for ε-caprolactone polymerisation at 80°C.

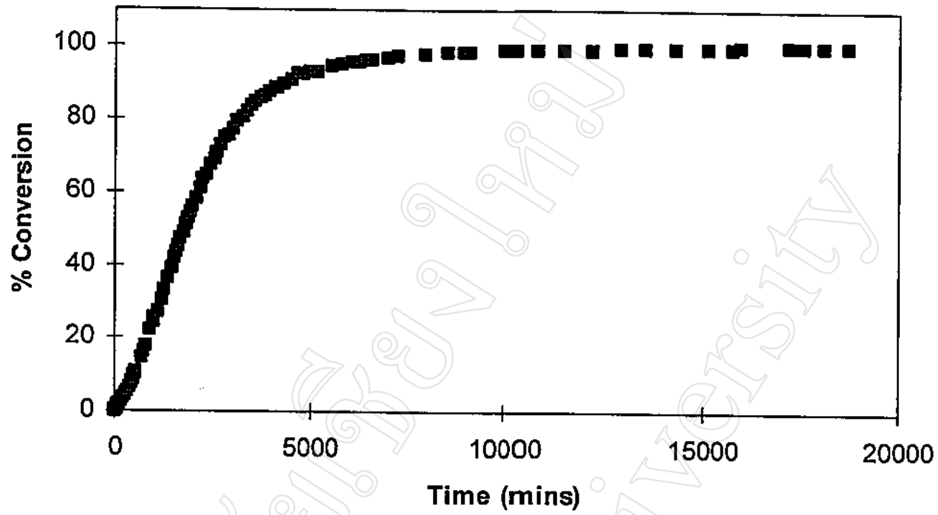

Fig. 4.12 : Kinetic profile from dilatometry of % conversion against time for ε-caprolactone polymerisation at 80°C.

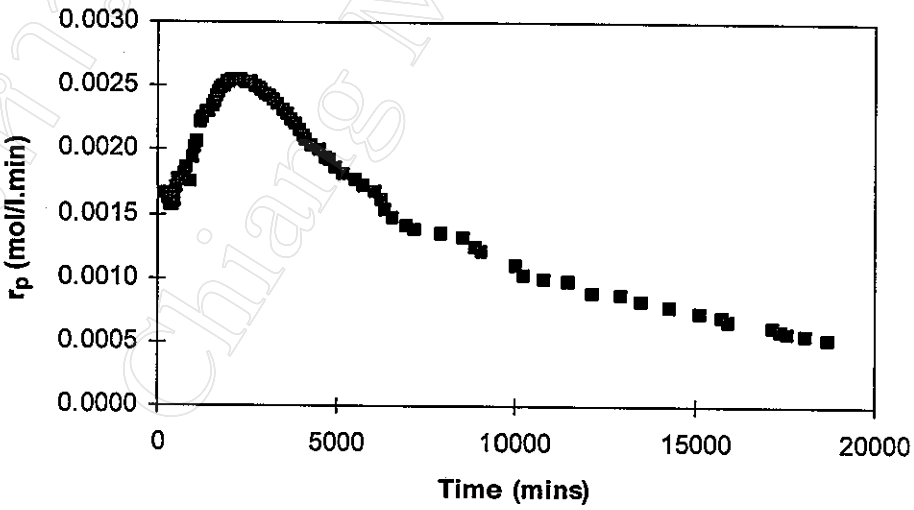

Fig. 4.13 : Kinetic profile from dilatometry of the rate of polymerisation, r_p , against time for ε-caprolactone polymerisation at 80°C.

Table 4.4 : Dilatometric data from ε-caprolactone polymerisation at 90°C.

weight of ε-caprolactone = 15.3746 g
weight of stannous octoate = 0.0547 g
capillary diameter = 0.143 cm
h_0 (from extrapolation in Fig. 4.15) = 25.030 cm

Time (mins)	h (cm)	Conversion (%)	r_p (mol/l·min)
2	24.640	thermal equilibration	
4	24.930		
5	24.960		
6	24.978		
7	25.000		
9	24.995	0.16	0.00154
11	24.995	0.16	0.00126
12	24.975	0.24	0.00181
20	24.952	0.35	0.00154
25	24.905	0.55	0.00198
30	24.925	0.47	0.00138
45	24.850	0.80	0.00158
60	24.840	0.84	0.00125
75	24.795	1.04	0.00124
90	24.640	1.73	0.00171
105	24.604	1.89	0.00160
115	24.515	2.29	0.00177
120	24.465	2.51	0.00186
135	24.240	3.51	0.00231
150	24.140	3.95	0.00235
165	23.986	4.63	0.00250
180	23.840	5.28	0.00262
195	23.620	6.26	0.00286
210	23.535	6.64	0.00282
225	23.340	7.50	0.00297
240	23.000	9.01	0.00335
255	22.945	9.25	0.00323
275	22.650	10.56	0.00342
285	22.480	11.32	0.00354
300	22.300	12.12	0.00360
315	22.085	13.07	0.00370
330	21.835	14.18	0.00383
345	21.625	15.11	0.00390
360	21.420	16.02	0.00397
375	21.215	16.93	0.00402
400	20.875	18.44	0.00411
405	20.875	18.44	0.00406
420	20.550	19.88	0.00422
435	20.320	20.91	0.00428
450	20.100	21.88	0.00433
480	19.670	23.79	0.00442
510	19.220	25.79	0.00451
540	18.750	27.87	0.00460
570	18.290	29.92	0.00468
600	17.800	32.09	0.00477
630	17.350	34.09	0.00482
660	16.820	36.44	0.00492
690	16.179	39.29	0.00507

Table 4.4 : continued

Time (mins)	h (cm)	Conversion (%)	r_p (mol/l·min)
710	16.075	39.75	0.00499
720	15.870	40.66	0.00503
750	15.470	42.43	0.00504
780	15.010	44.47	0.00508
810	14.550	46.52	0.00512
840	14.100	48.51	0.00515
900	13.294	52.09	0.00516
940	12.740	54.55	0.00517
955	12.504	55.60	0.00519
1010	11.765	58.88	0.00520
1080	10.950	62.49	0.00516
1140	10.185	65.89	0.00515
1200	9.575	68.60	0.00509
1240	9.009	71.11	0.00511
1320	8.475	73.48	0.00496
1325	8.330	74.12	0.00499
1380	7.880	76.12	0.00492
1440	7.350	78.47	0.00486
1500	6.925	80.36	0.00477
1560	6.550	82.02	0.00469
1620	6.200	83.58	0.00460
1680	5.890	84.95	0.00451
1740	5.520	86.60	0.00444
1800	5.265	87.73	0.00434
1840	5.002	88.89	0.00431
1940	4.740	90.06	0.00414
1980	4.675	90.35	0.00407
2040	4.480	91.21	0.00398
2190	4.150	92.68	0.00377
2220	4.060	93.08	0.00374
2280	3.965	93.50	0.00365
2370	3.760	94.41	0.00355
2520	3.575	95.23	0.00337
2640	3.470	95.69	0.00323
2760	3.330	96.32	0.00311
2820	3.255	96.65	0.00305
2880	3.226	96.78	0.00299
3060	2.975	97.89	0.00285
3300	2.975	97.89	0.00264
3480	2.885	98.29	0.00252
3720	2.790	98.71	0.00237
4260	2.700	99.11	0.00207
4440	2.725	99.00	0.00199
4860	2.675	99.22	0.00182
5230	2.625	99.45	0.00169
5700	2.560	99.73	0.00156
6000	2.550	99.78	0.00148
6180	2.550	99.78	0.00144
6270	2.550	99.78	0.00142
6480	2.550	99.78	0.00137
7110	2.500	100.00	0.00125
7320	2.500	100.00	0.00122
7860	2.500	100.00	0.00113
8580	2.500	100.00	0.00104
8640	2.500	100.00	0.00103

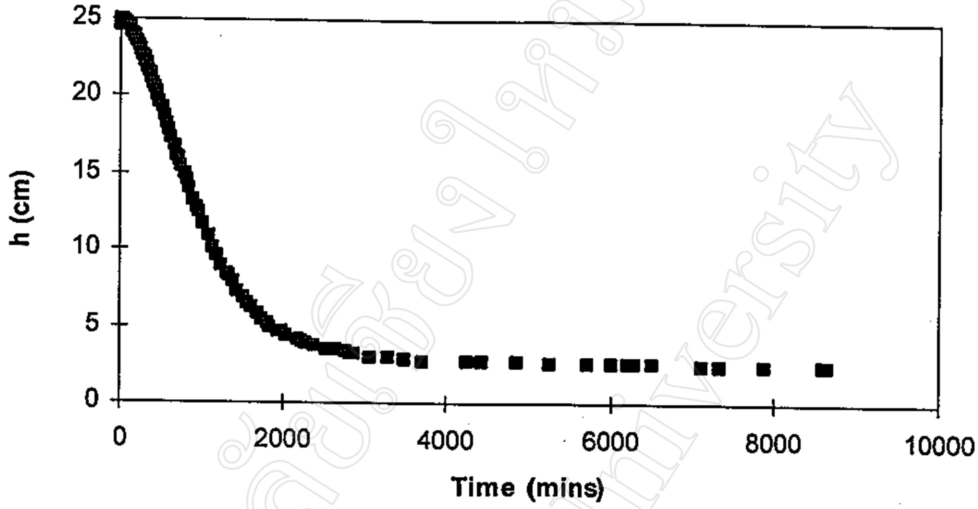

Fig. 4.14 : **Graph of meniscus height, h, against time for ε-caprolactone polymerisation at 90°C.**

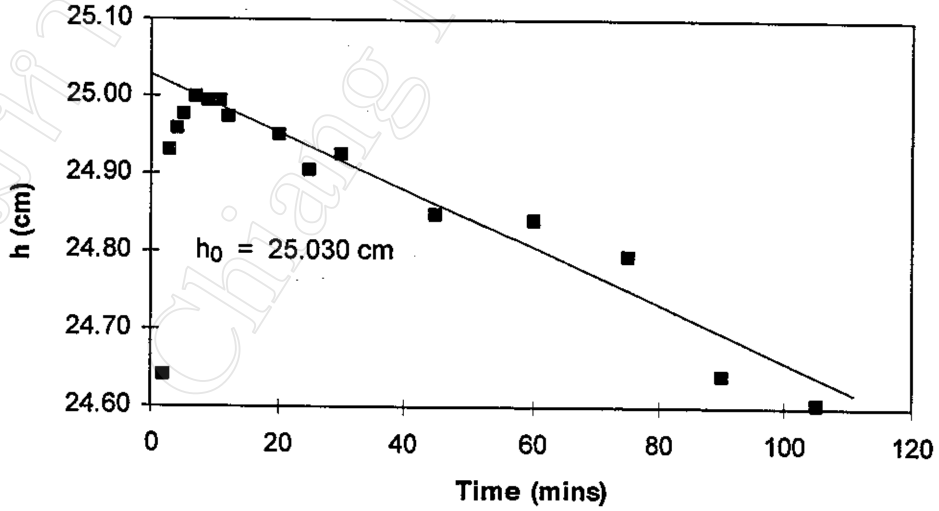

Fig. 4.15 : **Extrapolation of h to zero time (h_0 at t = 0) for ε-caprolactone polymerisation at 90°C.**

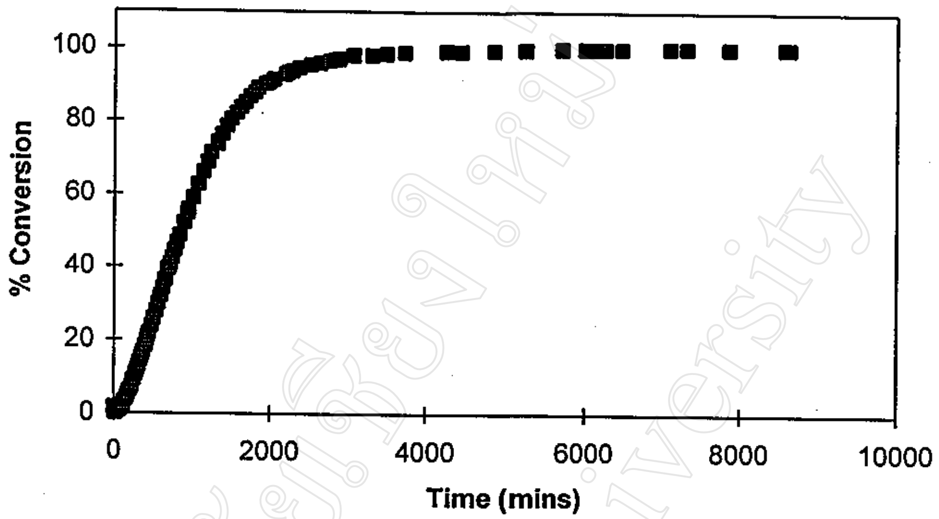

Fig. 4.16 : Kinetic profile from dilatometry of % conversion against time for ε-caprolactone polymerisation at 90°C.

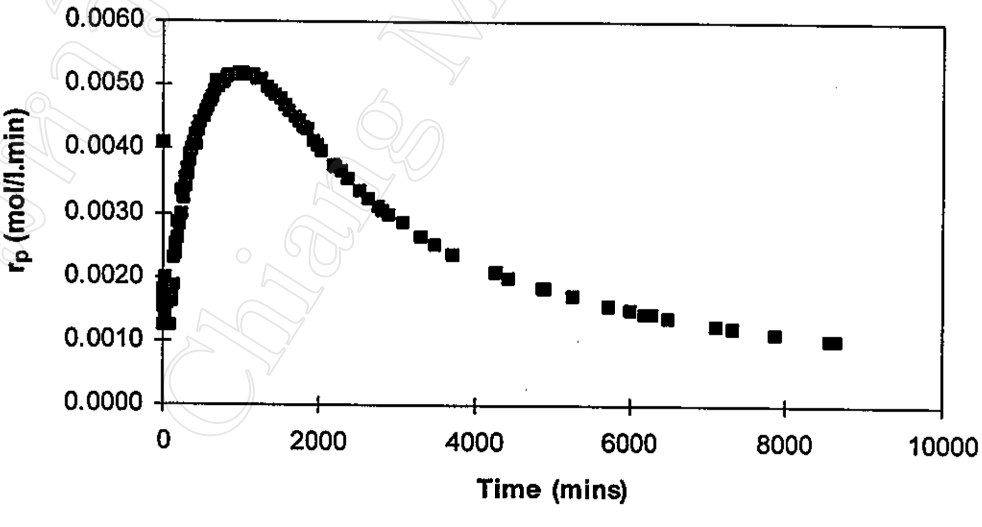

Fig. 4.17 : Kinetic profile from dilatometry of the rate of polymerisation, r_p , against time for ε-caprolactone polymerisation at 90°C.

4.1.3 Kinetic Analysis

From the previous results, the order of reaction, **n**, with respect to monomer can be investigated by plotting the appropriate rate function against time. Knowing the order of reaction, even if only approximately, can often yield valuable information regarding the nature of the polymerisation mechanism.

Cyclic ester polymerisations are usually reported in the literature as being first-order (n = 1) in monomer, following any induction period that may occur. However, zero-order (n = 0) kinetics have also been observed, for example in the bulk polymerisation of ε-caprolactone using triphenyltin acetate as initiator [127]. Consequently, in this work, both zero-order and first-order rate functions are plotted against time and the results compared for the first 20% conversion. Beyond this level of conversion, the increasing viscosity of the system leads to diffusion-controlled effects which, in turn, lead to deviations from simple-order kinetics.

The zero-order and first-order rate plots for the δ-valerolactone and ε-caprolactone polymerisations at 80°C and 90°C are compared in Figs. 4.18 - 4.25. The plots correspond to the following integrated forms of the general zero-order and first-order rate equations:

$$n = 0 \quad : \qquad [M]_0 - [M]_t \quad = \quad kt$$

$$n = 1 \quad : \qquad \ln\left([M]_0/[M]_t\right) \quad = \quad kt$$

in which the following correspondencies are assumed:

$$n = 0 \quad : \qquad [M]_0 - [M]_t \quad \alpha \quad \Delta h$$

$$n = 1 \quad : \qquad \ln\left([M]_0/[M]_t\right) \quad = \quad \ln\left(\Delta h[t = \infty]/\Delta h[t = \infty] - \Delta h\right)$$

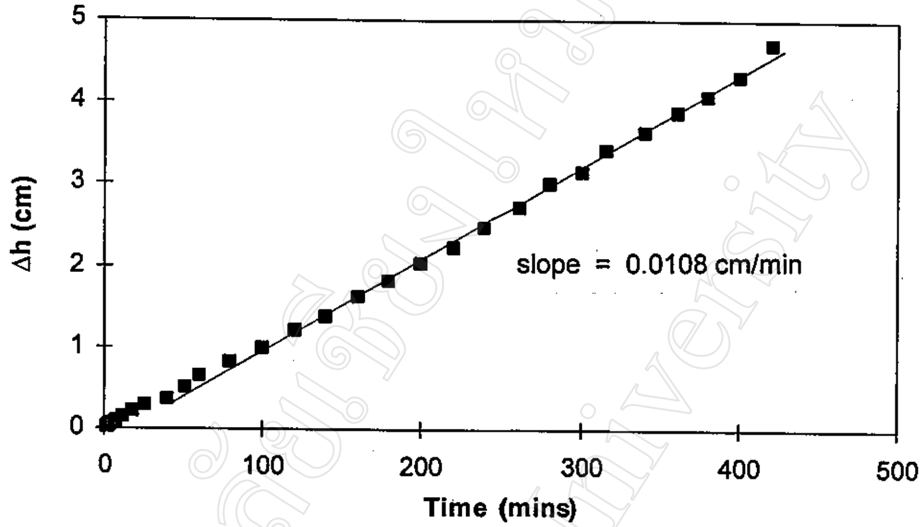

Fig. 4.18 : Zero-order rate plot from dilatometry for δ-valerolactone polymerisation at 80°C.

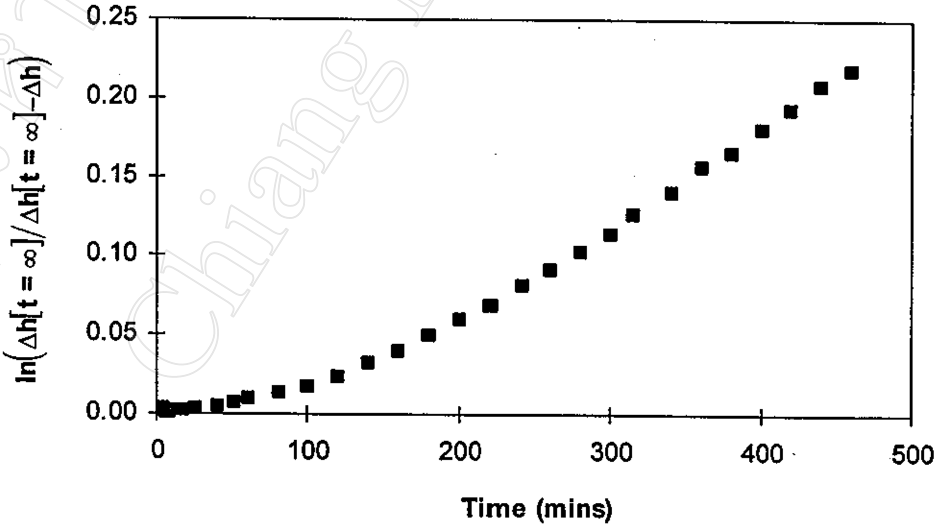

Fig. 4.19 : First-order rate plot from dilatometry for δ-valerolactone polymerisation at 80°C.

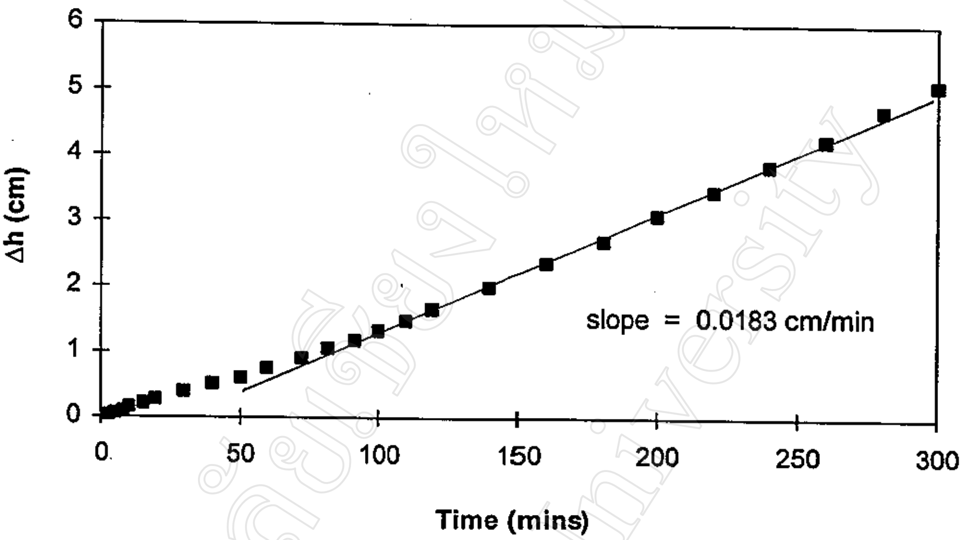

Fig. 4.20 : Zero-order rate plot from dilatometry for δ-valerolactone polymerisation at 90°C.

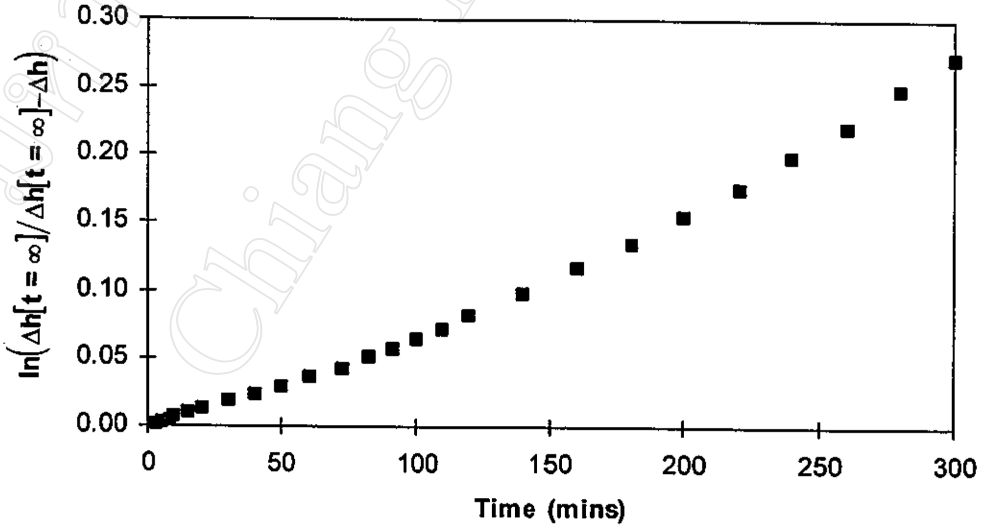

Fig. 4.21 : First-order rate plot from dilatometry for δ-valerolactone polymerisation at 90°C.

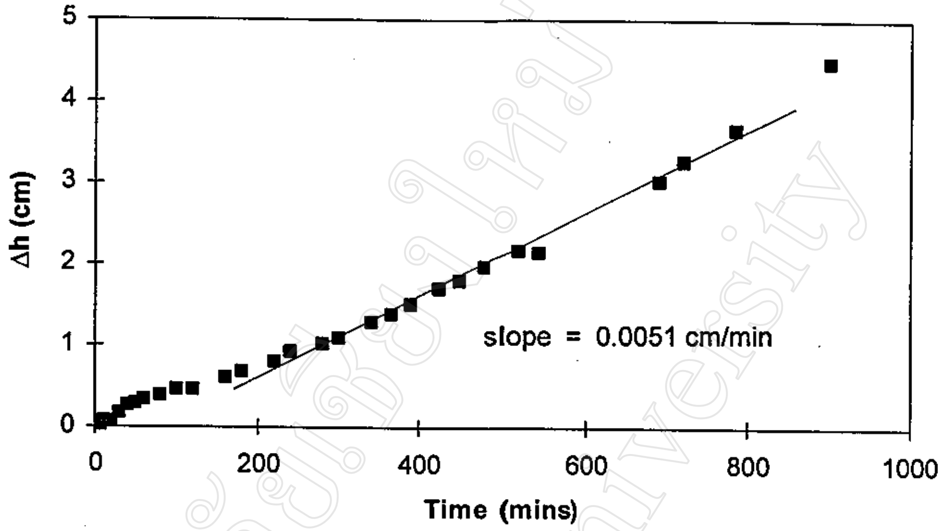

Fig. 4.22 : Zero-order rate plot from dilatometry for ε-caprolactone polymerisation at 80°C.

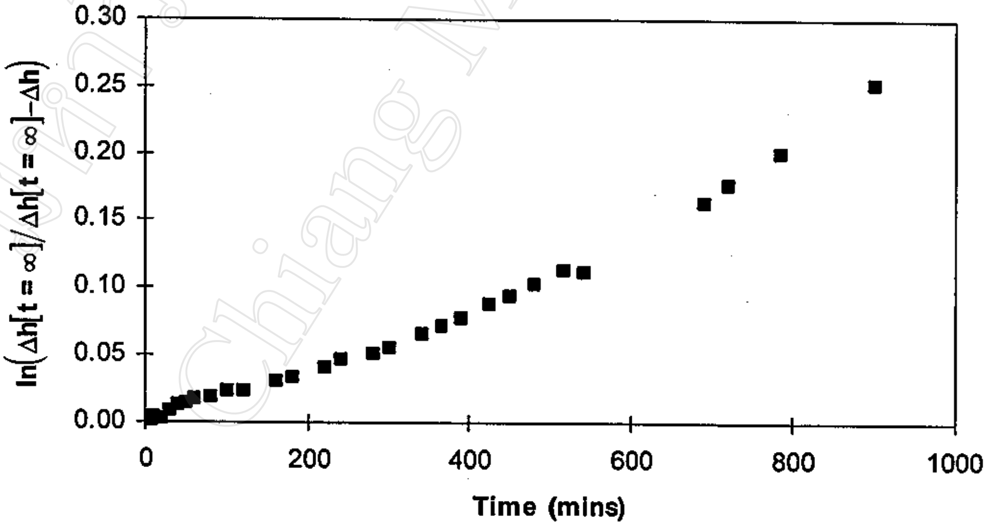

Fig. 4.23 : First-order rate plot from dilatometry for ε-caprolactone polymerisation at 80°C.

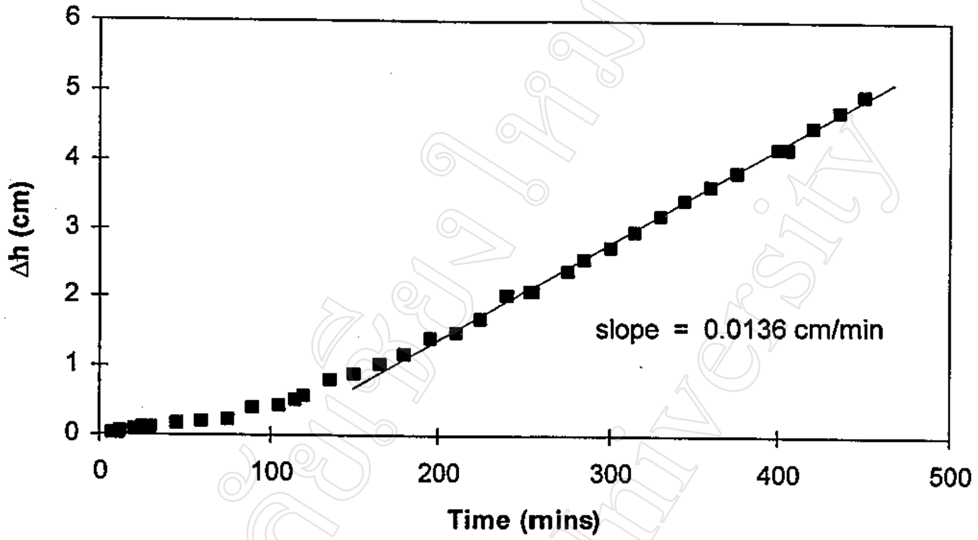

Fig. 4.24 : Zero-order rate plot from dilatometry for ε-caprolactone polymerisation at 90°C.

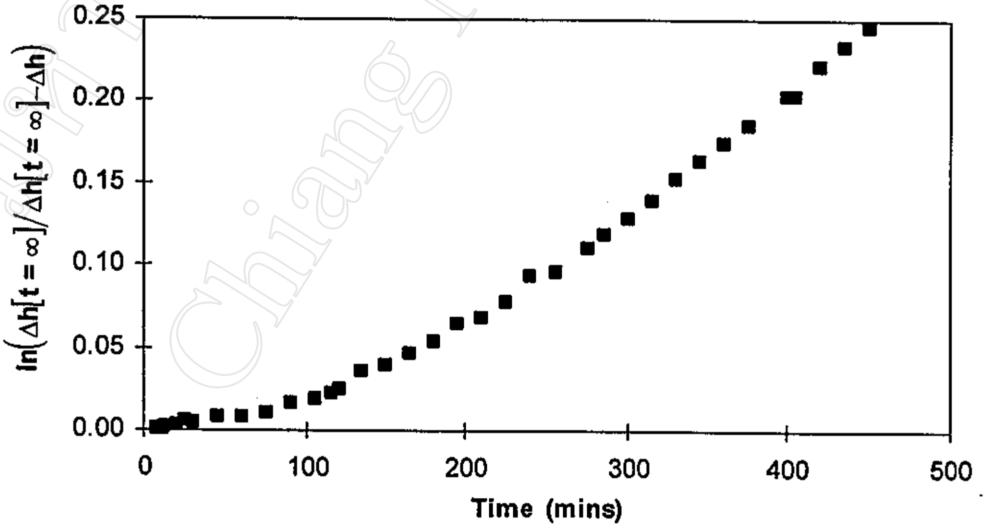

Fig. 4.25 : First-order rate plot from dilatometry for ε-caprolactone polymerisation at 90°C.

The resultant plots in Figs. 4.18-4.25 seem to indicate a closer adherence to zero-order than first-order kinetics, particularly after the first 10% conversion. The linear portions of the zero-order plots are preceded by what appear to be induction periods. The presence of an induction period in $Sn(Oct)_2$-initiated lactone polymerisation has variously been ascribed to the time taken for the complete dissolution and rearrangement of the coordinative aggregates of the $Sn(Oct)_2$ in the monomer, to the presence of trace moisture impurities in the system which may lead to the formation of less active $Sn(Oct)_2$ derivatives.

4.1.3.1 Zero-Order Rate Constants

From the linear portions of the zero-order rate plots, approximate values for the respective zero-order rate constants, k , can be calculated. According to the previous integrated rate expression:

$$[M]_0 - [M]_t = kt$$

where $[M]_0 - [M]_t \ \alpha \ \Delta h \quad (\text{or} = K\Delta h)$

thus $\Delta h = kt/K$

In these equations:

$[M]_0$ = initial monomer concentration at time t = 0

$[M]_t$ = remaining monomer concentration at time t

Δh = dilatometric change in meniscus height at time t

K = proportionality constant

k = zero-order rate constant

Since it is known that:

$[M]_o$ = concentration of pure monomer at the polymerisation temperature

and if it is assumed that the final limiting condition is:

$$[M]_t \rightarrow 0 \quad \text{at} \quad \Delta h\ (t = \infty)$$

then the value of the proportionality constant, K, can be calculated from:

$$[M]_0 \quad = \quad K\Delta h(t = \infty)$$

Knowing the value of K, the zero-order rate constant, k, can then be calculated from the slope ($\Delta h/t$) of the corresponding rate plot.

Following this methodology, the calculated values of $[M]_0$, $\Delta h(t{=}\infty)$, K, and k for each of the 4 kinetic experiments are listed in Table 4.5. As would be expected, the zero-order rate constant, k, increases with temperature but decreases with monomer ring size.

Also included at the bottom of Table 4.5 are the final % conversions, determined gravimetrically as described on page 206. Considering that the values are all over 90% and that, due to incomplete precipitation, the actual values are likely to be higher still, they lend justification to the assumption used in the kinetic analysis that $[M]_t \rightarrow 0$ at $\Delta h(t = \infty)$. This will be discussed further in the following section.

Table 4.5 : Comparison of the zero-order rate constants, k, and related kinetic parameters for the δ-valerolactone and ε-caprolactone polymerisations at 80°C and 90°C.

Kinetic Parameters	δ-valerolactone		ε-caprolactone	
	80°C	90°C	80°C	90°C
$[M]_0$, mol/l	10.522	10.433	8.988	8.913
Δh ($t = \infty$), cm	21.723	21.388	20.080	22.530
K, mol/l·cm	0.484	0.488	0.448	0.396
$k \times 10^3$, mol/l·min	5.23	8.93	2.28	5.36
% conversion ($t = \infty$) (from gravimetry)	90.6	94.7	94.8	97.5

4.2 Gravimetry

4.2.1 Experimental Procedure and Results

In contrast to the previous method of dilatometry which only provides indirect measurements of monomer conversion, gravimetry, in which the polymer produced is physically separated for quantitative determination, is the most direct way of obtaining conversion data. It does, however, suffer from the drawback that, in the course of separating the polymer formed from the residual monomer by dissolution and re-precipitation, the lowest molecular weight (oligomeric) fractions may not be able to precipitate as a filterable solid, leading to an erroneously low experimental value for the % conversion.

The polymerisation procedure used was the same as that described previously for dilatometry except that the reaction vessels were a series of tightly sealed, 7 ml, screw-top, glass sample bottles. At various time intervals during the polymerisation, a sample bottle was removed from the water bath, allowed to cool to room temperature, and its contents dissolved in chloroform. The polymer was then separated out from solution by dropwise addition into ice-cooled absolute ethanol with efficient stirring followed by prolonged standing to ensure the maximum amount of precipitation possible. Finally, the polymer precipitate was carefully filtered off under gentle suction in a sintered glass crucible (porosity 4), washed with more absolute ethanol, and dried to constant weight in a vacuum oven at room temperature (approx. 30°C).

From the dry weights of polymer obtained for both the δ-valerolactone and ε-caprolactone polymerisations at 80°C and 90°C, the % conversions were calculated as given in Tables 4.6-4.9. Also given are the corresponding number-average and weight-average molecular weights, $\overline{M}_n$ and $\overline{M}_w$, as determined by GPC.

4.2.2 Kinetic Analysis

The gravimetric % conversions in Tables 4.6-4.9 are plotted against time in Figs. 4.26-4.29 alongside the corresponding dilatometric data for comparison. The two types of data show significant differences with the % conversions from gravimetry being generally lower than those from dilatometry. The main reason for this disparity between the two techniques is, as mentioned previously, the likelihood of incomplete precipitation of the polymer in this gravimetric method. Indeed, according to the molecular weight data in Tables 4.6-4.9, it appears that neither polymer, PVL nor PCL could precipitate at values of $\overline{M}_n$ < 2000. This effect will inevitably cause the gravimetric % conversions to be *lower* than their true values. Another source of error which, conversely, causes the dilatometric % conversions to be slightly *higher* than their true values is the assumption of complete 100% conversion at Δh ($t = \infty$). This error is probably less serious than that from incomplete precipitation but, nevertheless, undoubtedly contributes to the disparity between the two sets of data.

However, despite these numerical differences, the overall kinetic profiles in Figs. 4.26-4.29 are similar in appearance for both methods. Even though gravimetry has the advantage of being the more direct method, it suffers from the greater disadvantage of being unresponsive during the initial build-up of molecular weight until such time that a critical molecular weight for precipitation is attained. Thereafter, it continues to underestimate the true % conversion due to the non-precipitation of the lowest molecular weight fractions. Consequently, from the experiments carried out here, the gravimetric data is less amenable to kinetic analysis than the dilatometric data.

Table 4.6 : Gravimetric % conversions and GPC molecular weight data from δ-valerolactone polymerisation at 80°C.

Monomer (g)	Initiator (g)	Time (mins)	Conversion (%)	Mol. Wt. Averages	
				$\overline{M}_n$	$\overline{M}_w$
1.010	0.0040	1440	0.0	-	-
1.003	0.0041	2865	34.6	2195	3026
1.011	0.0039	4177	85.7	3527	5180
1.011	0.0040	5700	86.8	6557	8477
1.008	0.0041	7082	87.6	8551	13860
1.007	0.0040	8570	84.6	7280	10610
1.011	0.0041	10088	86.2	5034	9404
1.002	0.0039	11520	83.2	5477	8231

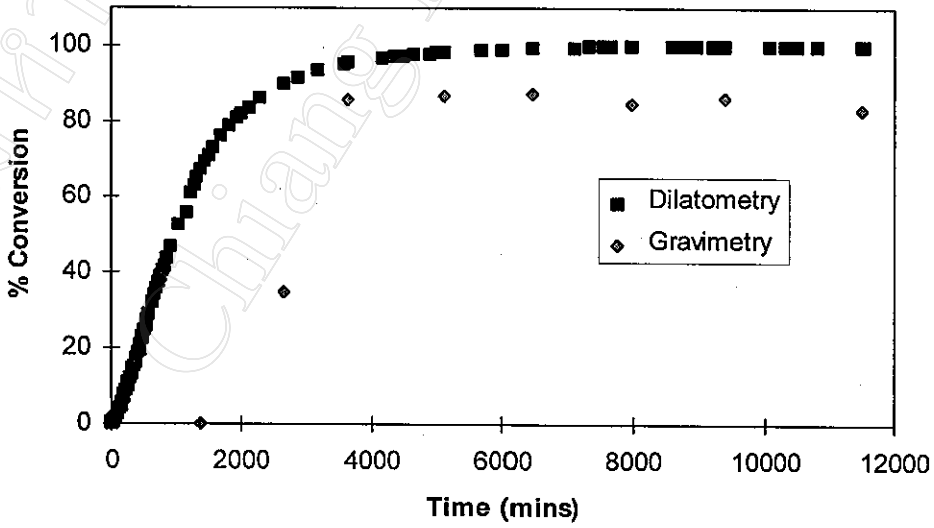

Fig. 4.26 : Comparison of gravimetric and dilatometric % conversion-time profiles for δ-valerolactone polymerisation at 80°C.

Table 4.7 : Gravimetric % conversions and GPC molecular weight data from δ-valerolactone polymerisation at 90°C.

Monomer (g)	Initiator (g)	Time (mins)	Conversion (%)	Mol. Wt. Averages	
				$\overline{M}_n$	$\overline{M}_w$
1.008	0.0041	360	0.0	-	-
1.007	0.0010	720	0.0	-	-
1.000	0.0040	1440	28.0	3700	4602
1.000	0.0039	2157	50.4	3738	4647
1.012	0.0041	2795	84.4	5879	8298
1.011	0.0039	3480	81.4	6411	12690
1.008	0.0039	4330	84.9	6837	11920
1.008	0.0040	5075	83.3	7641	11670
1.006	0.0040	5760	85.0	7362	11830

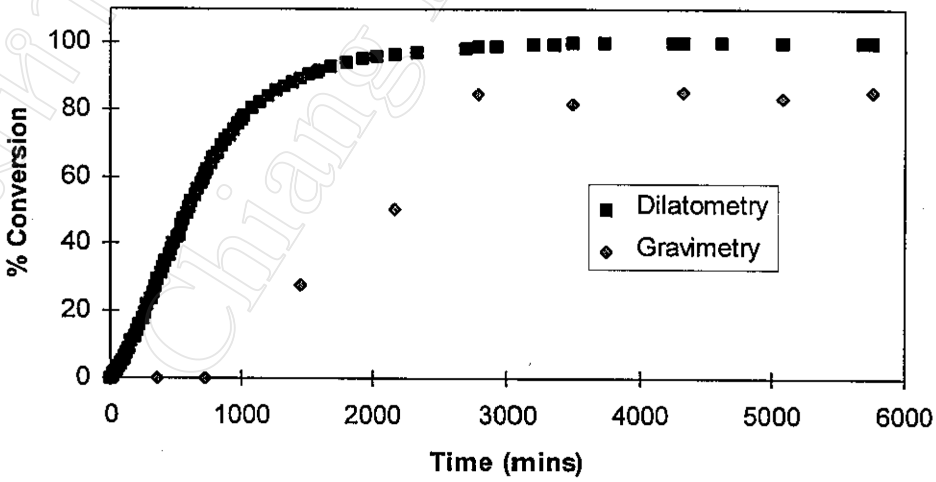

Fig. 4.27 : Comparison of gravimetric and dilatometric % conversion-time profiles for δ-valerolactone polymerisation at 90°C.

Table 4.8 : Gravimetric % conversions and GPC molecular weight data from ε-caprolactone polymerisation at 80°C.

Monomer (g)	Initiator (g)	Time (mins)	Conversion (%)	Mol. Wt. Averages	
				$\overline{M}_n$	$\overline{M}_w$
1.124	0.0039	4320	0.0	-	-
1.124	0.0040	5790	0.0	-	-
1.132	0.0040	7230	70.4	5549	7253
1.123	0.0039	10020	86.8	5733	7601
1.123	0.0040	11450	92.8	8642	11250
1.134	0.0041	12915	86.0	7241	11380
1.141	0.0040	14315	81.4	7408	10750
1.131	0.0040	15745	90.7	7620	11370
1.128	0.0040	17195	84.4	6344	9259
1.135	0.0040	18720	86.6	11250	16860

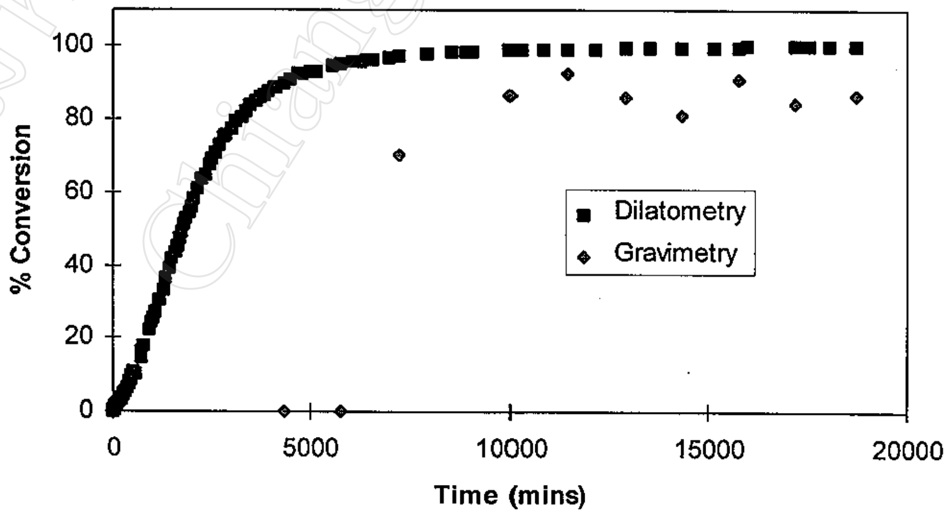

Fig. 4.28 : Comparison of gravimetric and dilatometric % conversion-time profiles for ε-caprolactone polymerisation at 80°C.

Table 4.9 : Gravimetric % conversions and GPC molecular weight data from ε-caprolactone polymerisation at 90°C.

Monomer (g)	Initiator (g)	Time (mins)	Conversion (%)	Mol. Wt. Averages	
				$\overline{M}_n$	$\overline{M}_w$
1.128	0.0039	1440	0.0	-	-
1.129	0.0039	2880	0.0	-	-
1.123	0.0039	4320	73.8	3030	4157
1.130	0.0039	6000	88.2	9707	14960
1.129	0.0039	8640	92.2	7560	12220

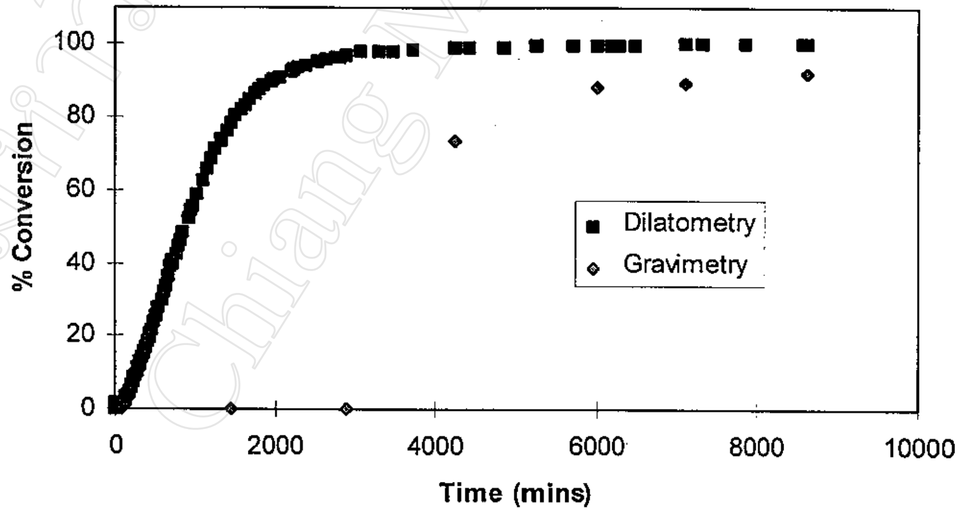

Fig. 4.29 : Comparison of gravimetric and dilatometric % conversion-time profiles for ε-caprolactone polymerisation at 90°C.

4.3 Viscosity

4.3.1 Experimental Procedure and Results

One of the most important features of polymerisation reactions is the large increase in viscosity with monomer conversion. The viscosity of the reaction mass may increase by several orders of magnitude, particularly in homogeneous systems such as bulk polymerisation.

In this study, the distilled monomer and 0.1 mole % of stannous octoate initiator were weighed out accurately and placed in a calibrated Ubbelohde suspended-level viscometer of the type shown previously in Fig. 2.50 (page 102). The viscometer was then clamped vertically in a thermostatically controlled water bath at the appropriate temperature and the polymerisation reaction allowed to proceed *in situ*. As the system polymerised, the increase in viscosity was measured in terms of the viscometric **flow-time** (s). This flow-time was then converted into units of viscosity (cS) via the viscometer's viscosity constant (0.01 cS/s).

The viscometry results obtained for both the δ-valerolactone and ε-caprolactone polymerisations at 80°C and 90°C are given in Tables 4.10-4.13 and the corresponding viscosity-time graphs plotted in Figs. 4.30-4.33. Also plotted alongside them for comparison are the previous % conversion curves from dilatometry so that the viscosity increases can be related to the actual reaction profiles.

Table 4.10 : Undiluted monomer-polymer viscometric data from δ-valerolactone polymerisation at 80°C.

Polymerisation Time (mins)	Flow-time (s)	Viscosity (cS)
0	124.8	1.248
120	138.0	1.380
240	156.1	1.561
360	174.9	1.749
480	189.9	1.899
600	205.0	2.050
720	217.7	2.177
840	230.8	2.308
960	242.9	2.429
1080	255.7	2.557
1200	269.4	2.694
1320	288.0	2.880
1440	305.4	3.054
1560	334.2	3.342
1680	365.6	3.656
1740	382.0	3.820
1800	407.5	4.075
1920	454.7	4.547
1980	490.4	4.904
2040	531.5	5.315
2160	629.5	6.295
2280	771.4	7.714
2400	965.5	9.655

Table 4.11 : Undiluted monomer-polymer viscometric data from δ-valerolactone polymerisation at 90°C.

Polymerisation Time (mins)	Flow-time (s)	Viscosity (cS)
0	111.4	1.114
120	133.2	1.332
240	195.4	1.954
300	237.1	2.371
360	280.5	2.805
420	331.1	3.311
480	398.1	3.981
540	477.3	4.773
600	571.1	5.711
660	660.5	6.605
720	754.1	7.541
780	851.7	8.517
840	936.9	9.369
900	1041.6	10.416
960	1143.7	11.437
1020	1262.4	12.624
1080	1409.6	14.096
1140	1569.6	15.696

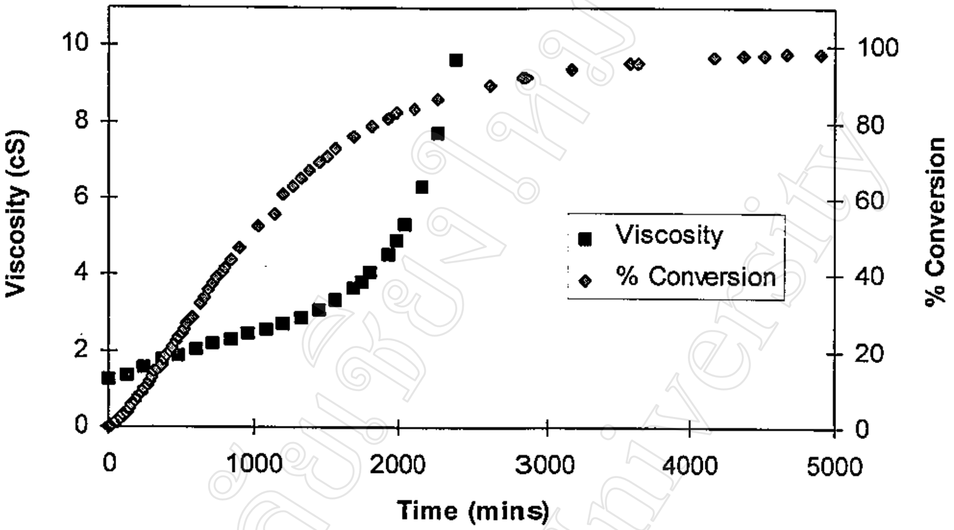

Fig. 4.30 : Comparison of the viscosity and % conversion-time profiles for δ-valerolactone polymerisation at 80°C.

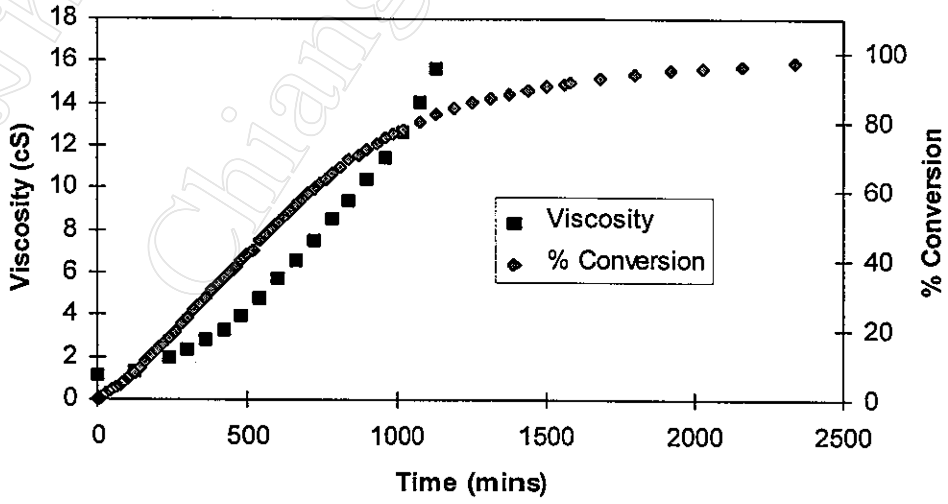

Fig. 4.31 : Comparison of the viscosity and % conversion-time profiles for δ-valerolactone polymerisation at 90°C.

Table 4.12 : Undiluted monomer-polymer viscometric data from ε-caprolactone polymerisation at 80°C.

Polymerisation Time (mins)	Flow-time (s)	Viscosity (cS)
0	198.3	1.983
120	191.1	1.911
240	191.9	1.919
420	193.0	1.930
660	193.8	1.938
780	194.6	1.946
960	194.6	1.946
1140	195.4	1.954
1320	196.7	1.967
1500	197.2	1.972
1680	198.3	1.983
1860	199.4	1.994
2040	200.7	2.007
2220	201.6	2.016
2400	203.6	2.036
2580	204.9	2.049
2820	207.4	2.074
3000	209.2	2.092
3180	211.8	2.118
3360	214.9	2.149
3540	218.8	2.188
3720	224.7	2.247
3900	227.1	2.271
4080	230.4	2.304
4260	236.6	2.366
4440	242.7	2.427
4620	253.3	2.533
4800	261.7	2.617
4980	268.4	2.684
5160	281.8	2.818

Table : 4.12 : continued

Polymerisation Time (mins)	Flow-time (s)	Viscosity (cS)
5700	343.1	3.431
5880	376.3	3.763
6060	411.3	4.113
6240	471.0	4.710
6360	521.3	5.213
6480	573.6	5.736
6600	623.9	6.239
6960	1018.2	10.182
7200	1404.4	14.044

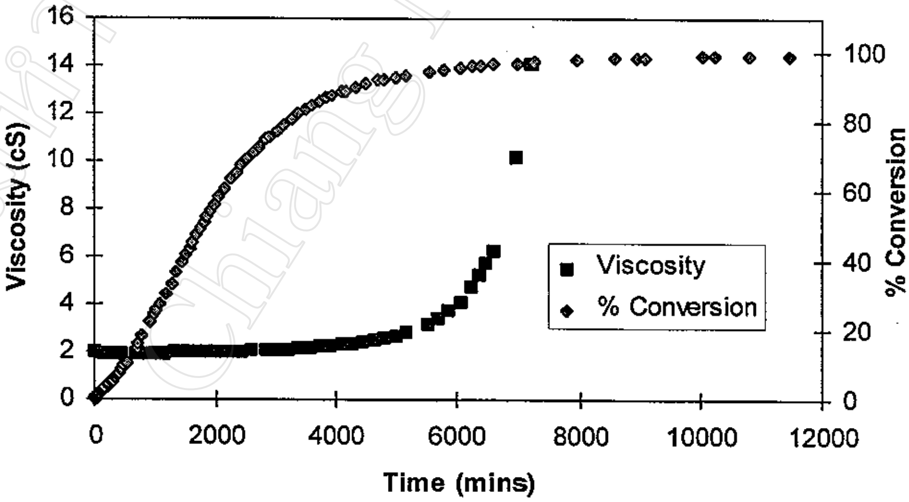

Fig. 4.32 : Comparison of the viscosity and % conversion-time profiles for ε-caprolactone polymerisation at 80°C.

Table 4.13 : Undiluted monomer-polymer viscometric data from ε-caprolactone polymerisation at 90°C.

Polymerisation Time (mins)	Flow-time (s)	Viscosity (cS)
0	164.0	1.640
60	166.8	1.668
120	169.0	1.690
180	170.5	1.705
240	171.9	1.719
360	174.6	1.746
420	179.2	1.792
540	181.9	1.819
780	186.7	1.867
1320	192.5	1.925
1440	194.5	1.945
1560	199.3	1.993
1680	207.4	2.074
1800	214.2	2.142
1920	232.3	2.323
2040	253.1	2.531
2160	276.8	2.768
2220	312.1	3.121
2340	359.8	3.598
2460	469.6	4.696
2580	611.5	6.115
2700	971.6	9.716
2760	1116.4	11.164
2820	1336.6	13.366
2940	1535.6	15.356
3000	2017.6	20.176

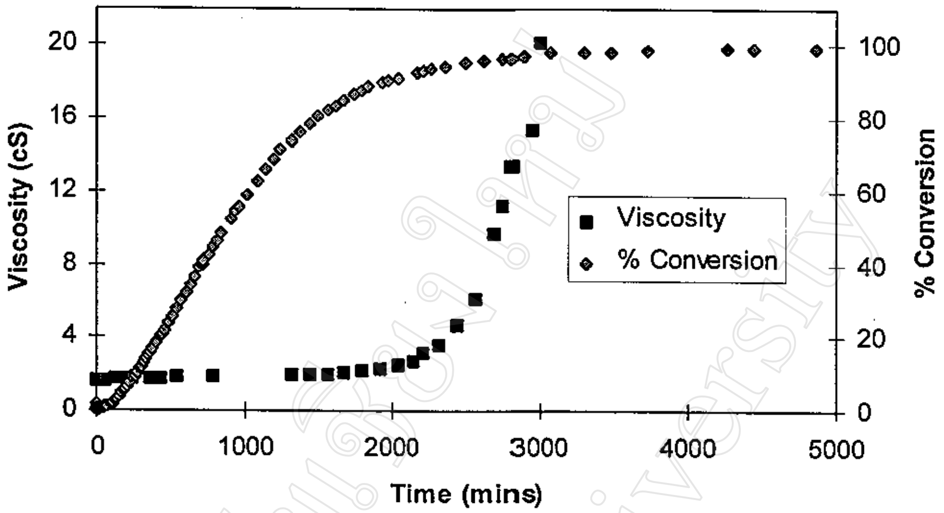

Fig. 4.33 : Comparison of the viscosity and % conversion-time profiles for ε-caprolactone polymerisation at 90°C.

4.3.2 Kinetic Analysis

As described previously in section 2.3.9.2 on pages 107-110, the relationship between molecular weight M and viscosity η_o of undiluted polymeric liquids is given by the empirical equation:

$$\eta_o \quad = \quad KM^a$$

where K and a are constants.

If we consider that, in the experiments conducted here, the pure monomer at time t = 0 is equivalent to the polymer of degree of polymerisation DP = 1, then the polymerising system as a whole can be regarded as an undiluted polymeric liquid of increasing average molecular weight. Thus, the previous viscosity-time curves in Figs. 4.30-4.33 are analogous to viscosity-molecular weight curves, although the precise molecular weight-time correspondence is unknown.

When the viscosity-time data is plotted logarithmically, as shown in Figs. 4.34-4.37, graphs are obtained which resemble the log η_o - log M plot in Fig. 2.53 (page 108). The viscosity undergoes an abrupt increase at a stage of the reaction which is generally attributed to the attainment of a certain "critical molecular weight" M_C. This M_C, which is structure-dependent, has been identified [113, 114] with M_o, the molecular weight between points of entanglement coupling, through the approximate relationship $M_C \approx 2M_o$. From the tangent line constructions in Figs. 4.34-4.37, the various "critical" reaction parameters associated with the sudden increases in viscosity are compared in Table 4.14.

Table 4.14 : Comparison of the reaction parameters at the critical condition for viscosity increase in the polymerisations of δ-valerolactone and ε-caprolactone at 80°C and 90°C from undiluted monomer-polymer viscometry.

Polymerisation Reaction	**Reaction Parameters at Critical Condition**			
	Viscosity η_C (cS)	**Time t_C (mins)**	**Conversion[a] %**	**Mol. Wt.[b] M_C**
δ-valerolactone @ 80°C	2.90	1700	76.0	2000
δ-valerolactone @ 90°C	*ind*	*ind*	*ind*	*ind*
ε-caprolactone @ 80°C	2.04	5900	95.4	5000
ε-caprolactone @ 90°C	1.95	2800	96.7	< 3000

a estimated % conversion from dilatometry

b estimated $\overline{M}_n$ (GPC) of polymer from gravimetry

ind indeterminable from the points in Fig. 4.35

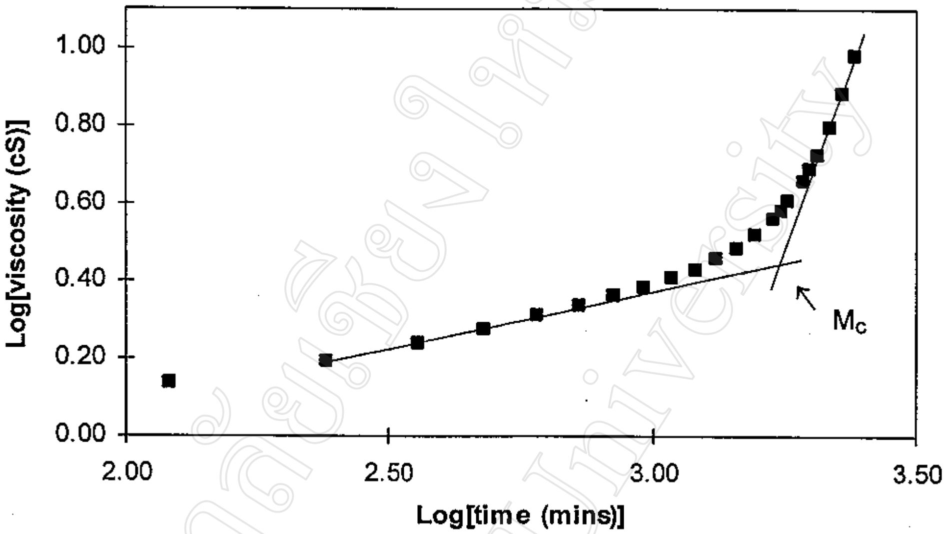

Fig. 4.34 : Logarithmic viscosity-time plot for undiluted (bulk) δ-valerolactone polymerisation at 80°C.

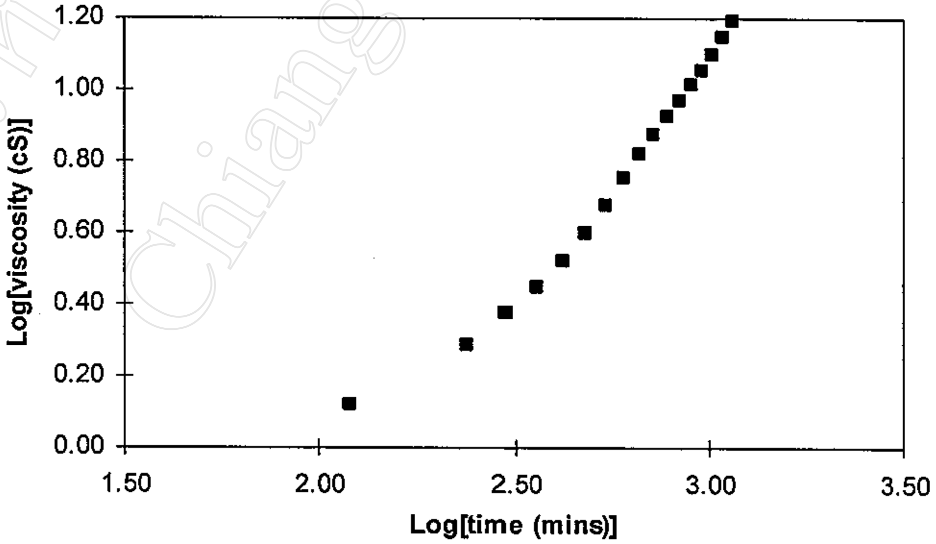

Fig. 4.35 : Logarithmic viscosity-time plot for undiluted (bulk) δ-valerolactone polymerisation at 90°C.

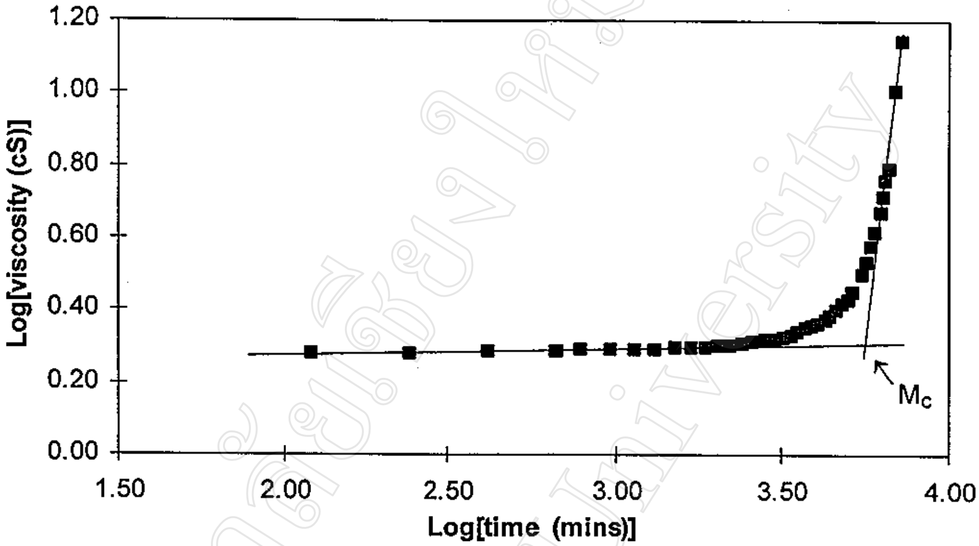

Fig. 4.36 : Logarithmic viscosity-time plot for undiluted (bulk) ε-caprolactone polymerisation at 80°C.

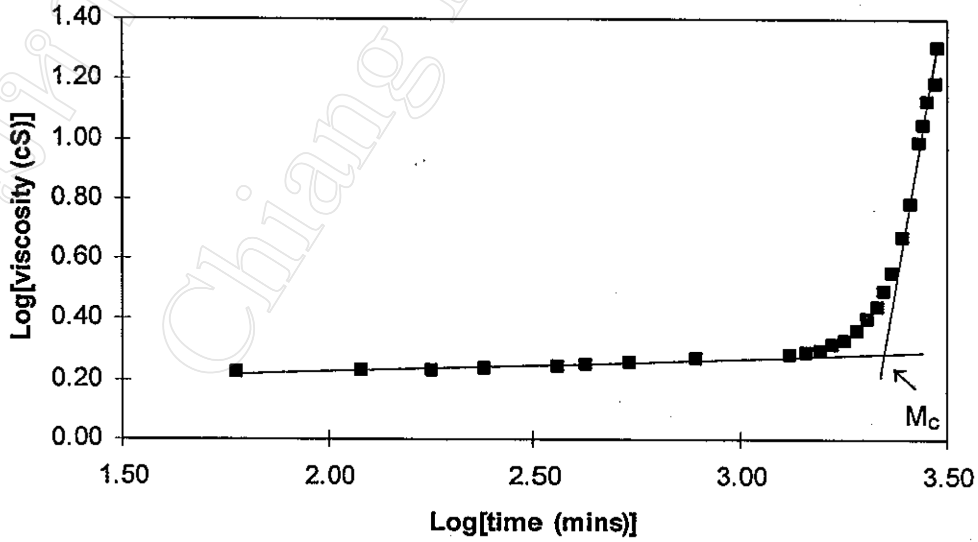

Fig. 4.37 : Logarithmic viscosity-time plot for undiluted (bulk) ε-caprolactone polymerisation at 90°C.

While the results in Table 4.14 are interesting, they need to be interpreted with caution. This is because, just as the polymerising system can be considered as a "*polymeric liquid*" starting from DP = 1 at time t = 0, strictly speaking, it can also be considered as a "*polymer solution*" in monomer starting from concentration c = 0 at time t = 0. Thus, there will be overlapping contributions to the overall viscosity increase from both the increasing $\overline{DP}$ (molecular weight) and the increasing concentration (% conversion). The extent to which these contributions can be differentiated, if at all, depends on the nature and mechanism of the reaction and the value of M_c.

From the log(viscosity)-log(time) plots in Figs. 4.34-4.37, the fact that they do show abrupt increases in viscosity, similar to the log(viscosity)-log(mol. wt.) plot in Fig. 2.53/page 108, suggest that the sudden change, when it occurs, is more a molecular weight than a conversion effect. The high conversion at which it occurs (> 95% conversion for ε-caprolactone), supports this view. Indeed, the ε-caprolactone plots in Fig. 4.36 and 4.37 show very slow increases in viscosity up to nearly complete conversion, resembling molecular weight-time plots in a stepwise polymerisation. This resemblance, when considered alongside the previous kinetic data, is perhaps a clue as to the nature of the polymerisation reaction. This and the other main points to arise from this kinetics section are now considered in conjunction with each other and the main conclusions summarized.

4.4 Main Conclusions

Although this Chapter 4 has been concerned with kinetics, it should be emphasized here that a complete elucidation of the kinetic nature of cyclic ester polymerisation has not been the main objective of this part of the work. Rather, the kinetic experiments conducted here, on just 2 chosen monomers, are merely intended to contribute to the overall discussion on the effect of ring size on lactone polymerisability and highlight possible areas for further work. From the results presented in this chapter, the main conclusions which can be drawn are as follows:

1. Under the reaction conditions employed, δ-valerolactone polymerises slightly faster than ε-caprolactone. This is consistent with the earlier results in Chapter 3 and is despite the greater ring strain in ε-caprolactone. This illustrates the point that, important though ring strain undoubtedly is, it is not necessarily the dominant factor in determining polymerisability, as measured in terms of rate. A whole range of other factors are important too, as described previously in section 1.4 (pages 14-28).

2. Kinetic analysis of the results from dilatometry appears to show a closer adherence to zero-order than first-order kinetics, particularly after the initial 10% conversion. However, the respective plots are not all that dissimilar and should not be taken as conclusive evidence of zero-order kinetics. Indeed, intuitively, the reaction is more likely to be first-order in monomer, as most homogeneous bulk cyclic ester polymerisations have been found to be. Deviations from the expected first-order kinetics may arise from oversimplifications in the dilatometric theory itself, such as (a) the assumption of complete (100%) conversion at Δh ($t = \infty$) and (b) the use of a constant factor, derived from the density of high polymer, to convert Δh to % conversion. While (a) may be reasonable to a good approximation (as confirmed here by gravimetry), (b) may seriously underestimate % conversion during the initial oligomeric stages of the reaction when density is still increasing with polymer molecular weight, as visualized below.

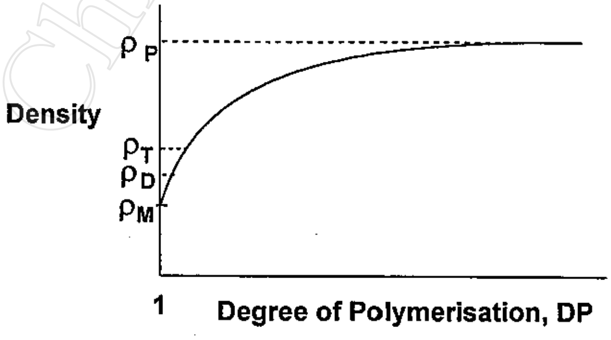

ρ_M = density of pure monomer

ρ_D = density of dimer

ρ_T = density of trimer

ρ_P = density of high polymer

Thus, the apparent adherence to zero-order kinetics observed here could be merely a fortuitious consequence of the true first-order nature of the reaction distorted by the deficiencies of the method. Elucidating this is a potential project in itself and, considering its importance in relation to the mechanism of the polymerisation, is an obvious area for further work.

3. Another practical effect which often leads to deviations from the underlying kinetic theory is ***autoacceleration*** resulting from the increase in viscosity of the system as the reaction proceeds. Mechanistically, this is interpreted in terms of a relative decrease in the termination rate as the molecular processes involved become diffusion-controlled, although this is usually for free radical rather than coordination-type polymerisations. In the dilatometry experiments carried out here, both δ-valerolactone and ε-caprolactone showed increases in rate, r_p, up to a maximum at around 50-60% conversion. This autoacceleration can also lead to an increase in temperature which then detracts from the isothermal nature of the experiment. Additionally, an increase in temperature due to the incomplete removal of the heat of reaction as the viscosity increases may lead to a "hot spot" and autoacceleration. These considerations, when taken together, lend weight to the suspicion that the apparent adherence to zero-order kinetics could be no more than an artefact of the method. The experimental deviations from the theory, not to mention the various dilatometer (viscosity, heat transfer) effects, are significant enough to undermine any firm conclusion as to the true order of the reaction.

4. Finally, the viscometry results suggested a gradual increase in molecular weight, more in common with a stepwise than an addition-type mechanism. When considered in conjunction with the previous conclusions, it therefore raises the question: could we be looking here at what are basically ***first-order stepwise growth*** polymerisations of which the kinetics are distorted by the various extraneous effects previously mentioned. The kinetic experiments described in this chapter are inadequate to answer this question. However, it does bring into sharp focus the need for a much more detailed kinetic study if this and other related mechanistic questions are to be answered.